SUPPLEMENTARY FIGURES

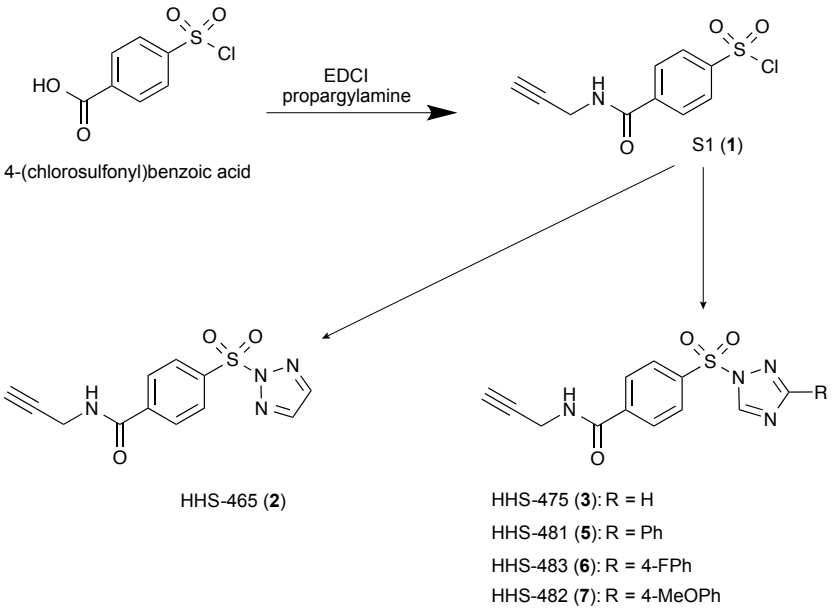

Supplementary Figure 1. Synthetic scheme showing general strategy for developing alkyne-modified sulfonyl-triazole probes.

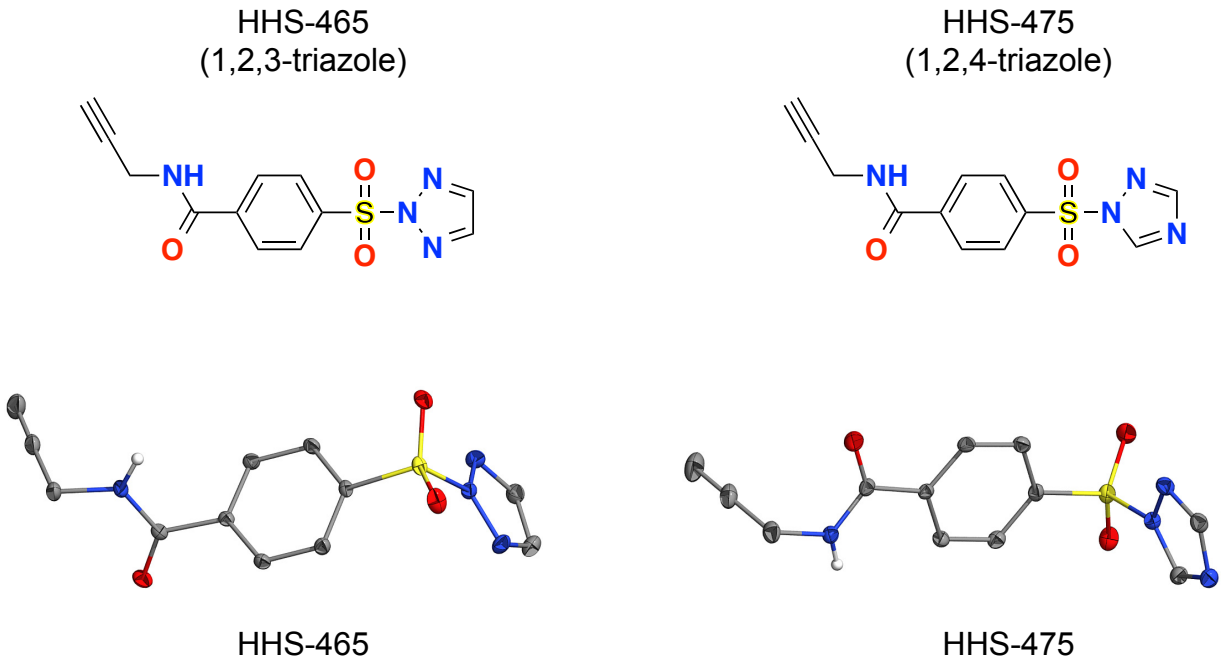

Supplementary Figure 2. Crystal structures of HHS-465 and HHS-475.

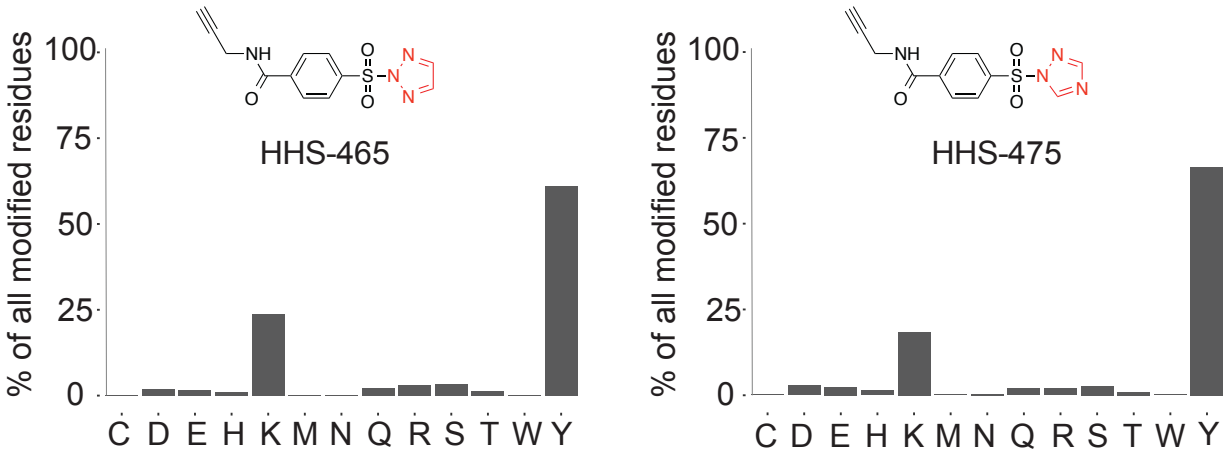

Supplementary Figure 3. Bar plot showing distribution of HHS-465 and HHS-475-modified sites (high confidence sites; Byonic score > 600) against nucleophilic amino acid residues detected in proteomes. Data shown are representative of two experiments (*n*=2 biologically independent experiments).

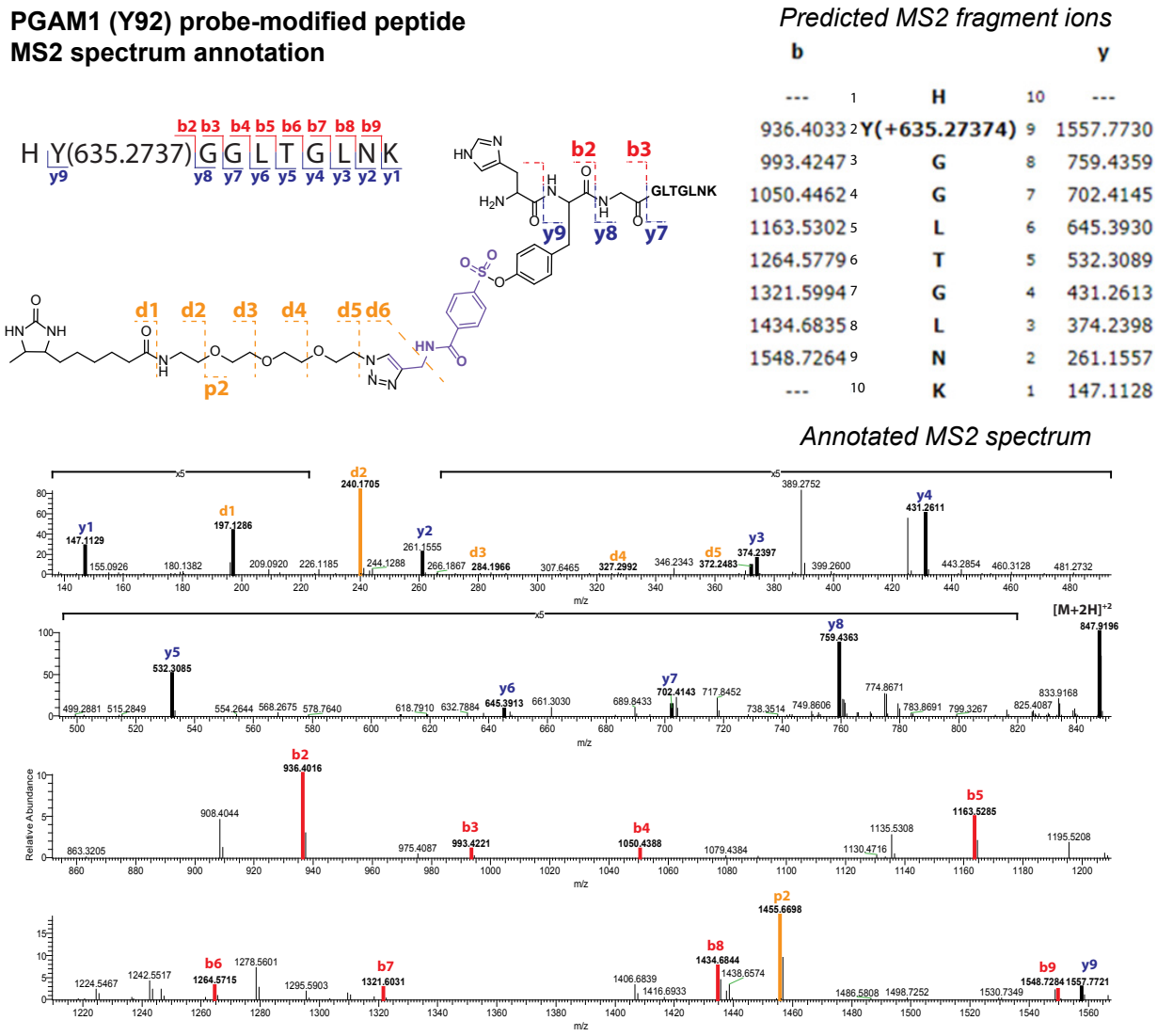

Supplementary Figure 4. **MS2 annotation of the PGAM1 (Y92) HHS-475-modified tryptic peptide**. Left panel: Modified sequence and fragment ion notation of HY*GGLTGLNK (residue 91-100) peptide from PGAM1. Covalent reaction of HHS-475 with Y92 results in a modified tyrosine (Y*) with the addition of +635.2737 Da. Fragmentation of the desthiobiotin-containing tag is also shown. Right panel: predicted MS2 b- and y-fragment ions from collision-induced dissociation (CID) as determined using Protein Prospector software (http://prospector.ucsf.edu/prospector/mshome.htm). Bottom panel: annotation of the MS2 spectrum for the HHS-475-modified PGAM1 Y92 tryptic peptide including fragment ions containing the probe binding site (modified tyrosine). Data shown are representative of two experiments (n=2 biologically independent experiments).

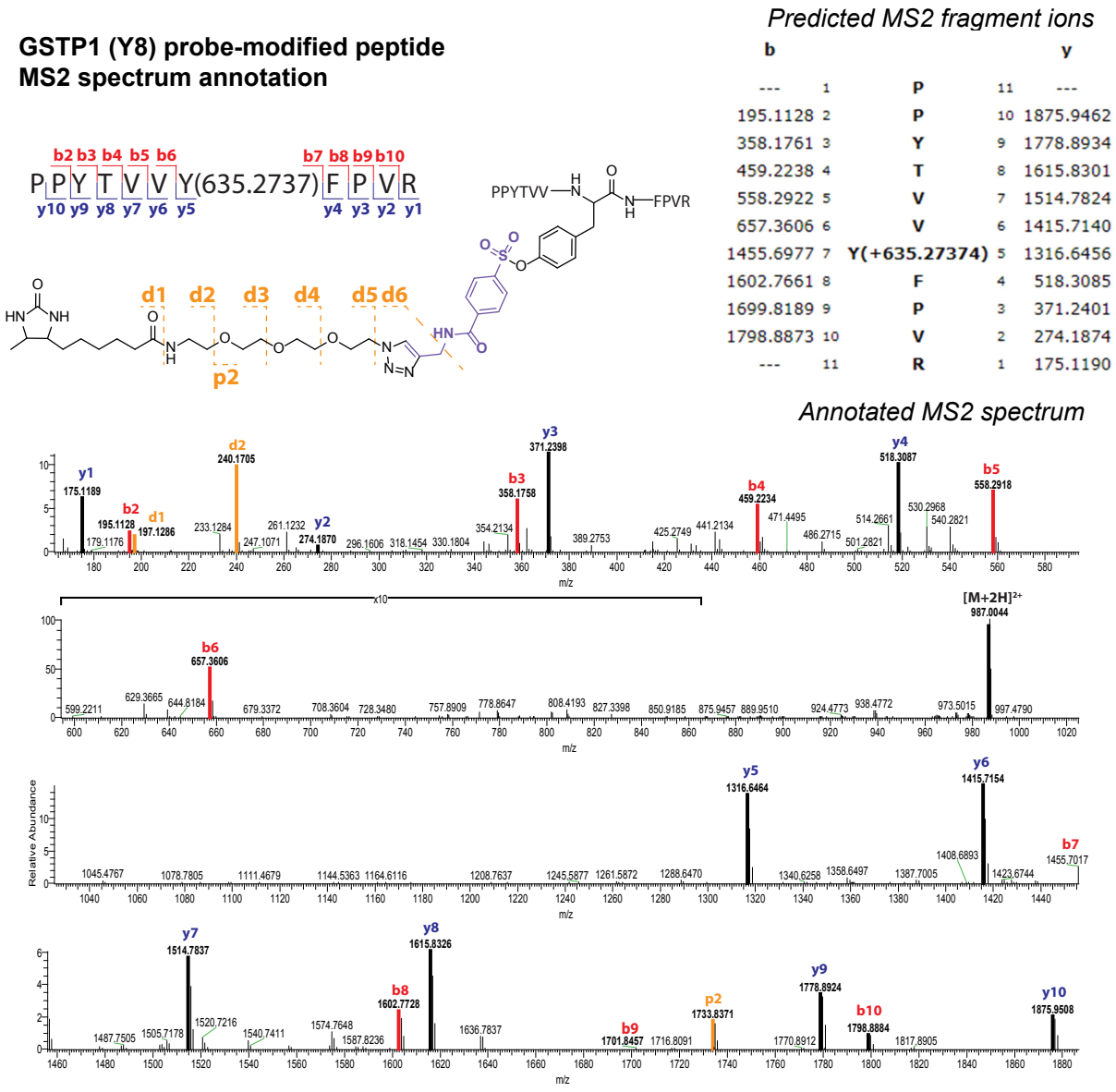

Supplementary Figure 5. MS2 annotation of the GSTP1 (Y8) HHS-475-modified tryptic peptide. Left panel: Modified sequence and fragment ion annotation of PPYTVVY*FPVR (residue 2-12) peptide from PGAM1. Covalent reaction of HHS-475 with Y8 results in a modified tyrosine (Y*) with the addition of +635.2737 Da. Fragmentation of the desthiobiotin-containing tag is also shown. Right panel: predicted MS2 b- and y-fragment ions from CID as determined using Protein Prospector software. Bottom panel: annotation of the MS2 spectrum for the HHS-475-modified GSTP1 Y8 tryptic peptide including fragment ions containing the probe binding site (modified tyrosine). Data shown are representative of two experiments (n=2 biologically independent experiments).

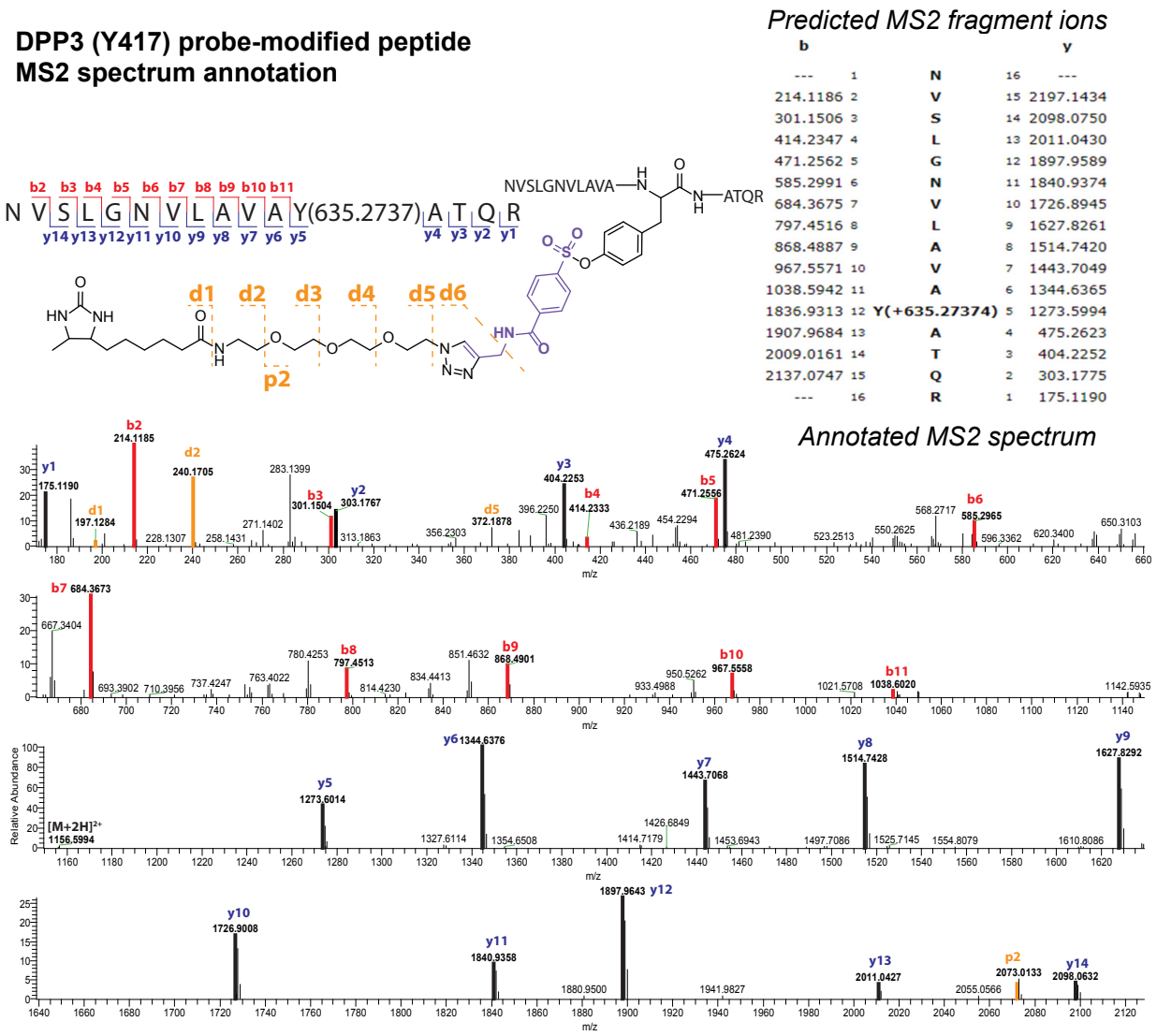

Supplementary Figure 6. **MS2 annotation of the DPP3 (Y417) HHS-475-modified tryptic peptide**. Left panel: Modified sequence and fragment ion notation of NVSLGNVLAVAY*ATQR (residue 406-421) peptide from DPP3. Covalent reaction of HHS-475 with Y417 results in a modified tyrosine (Y*) with the addition of +635.2737 Da. Fragmentation of the desthiobiotin-containing tag is also shown. Right panel: predicted MS2 b- and y-fragment ions from CID as determined using Protein Prospector software. Bottom panel: annotation of the MS2 spectrum for HHS-475-modified DPP3 Y417 tryptic peptide including fragment ions containing the probe binding site (modified tyrosine). Data shown are representative of two experiments (*n*=2 biologically independent experiments).

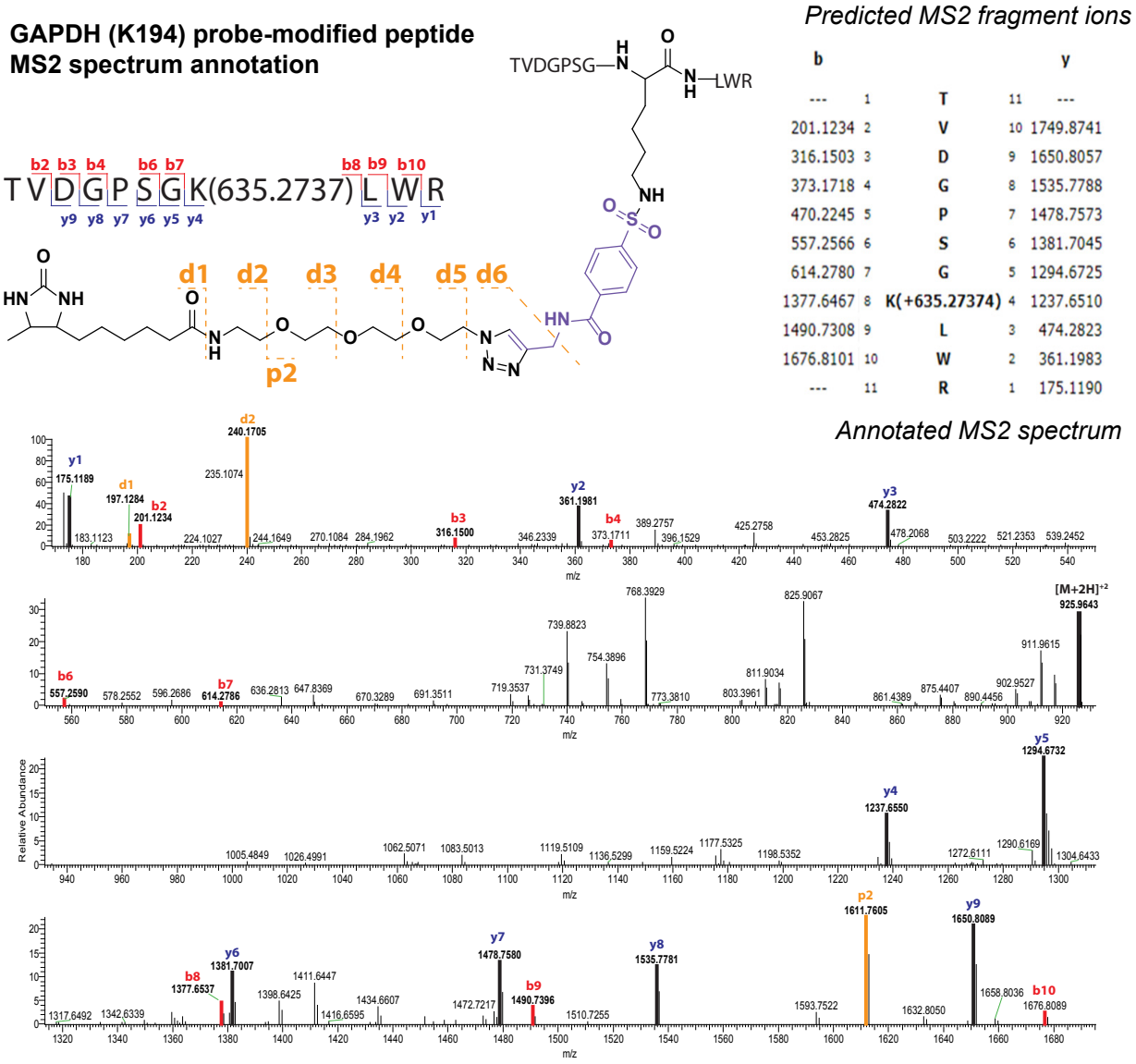

Supplementary Figure 7. **MS2 annotation of the GAPDH (K194) HHS-475-modified tryptic peptide**. Left panel: Modified sequence and fragment ion notation of TVDGPSGK*LWR (residue 187-197) peptide from GAPDH. Covalent reaction of HHS-475 with K194 results in a modified lysine (K*) with the addition of +635.2737 Da. Fragmentation of the desthiobiotin-containing tag is also shown. Right panel: predicted MS2 b- and y-fragment ions from CID as determined using Protein Prospector software. Bottom panel: annotation of the MS2 spectrum for HHS-475-modified GAPDH K194 tryptic peptide including fragment ions containing the probe binding site (modified lysine). Data shown are representative of two experiments (n=2 biologically independent experiments).

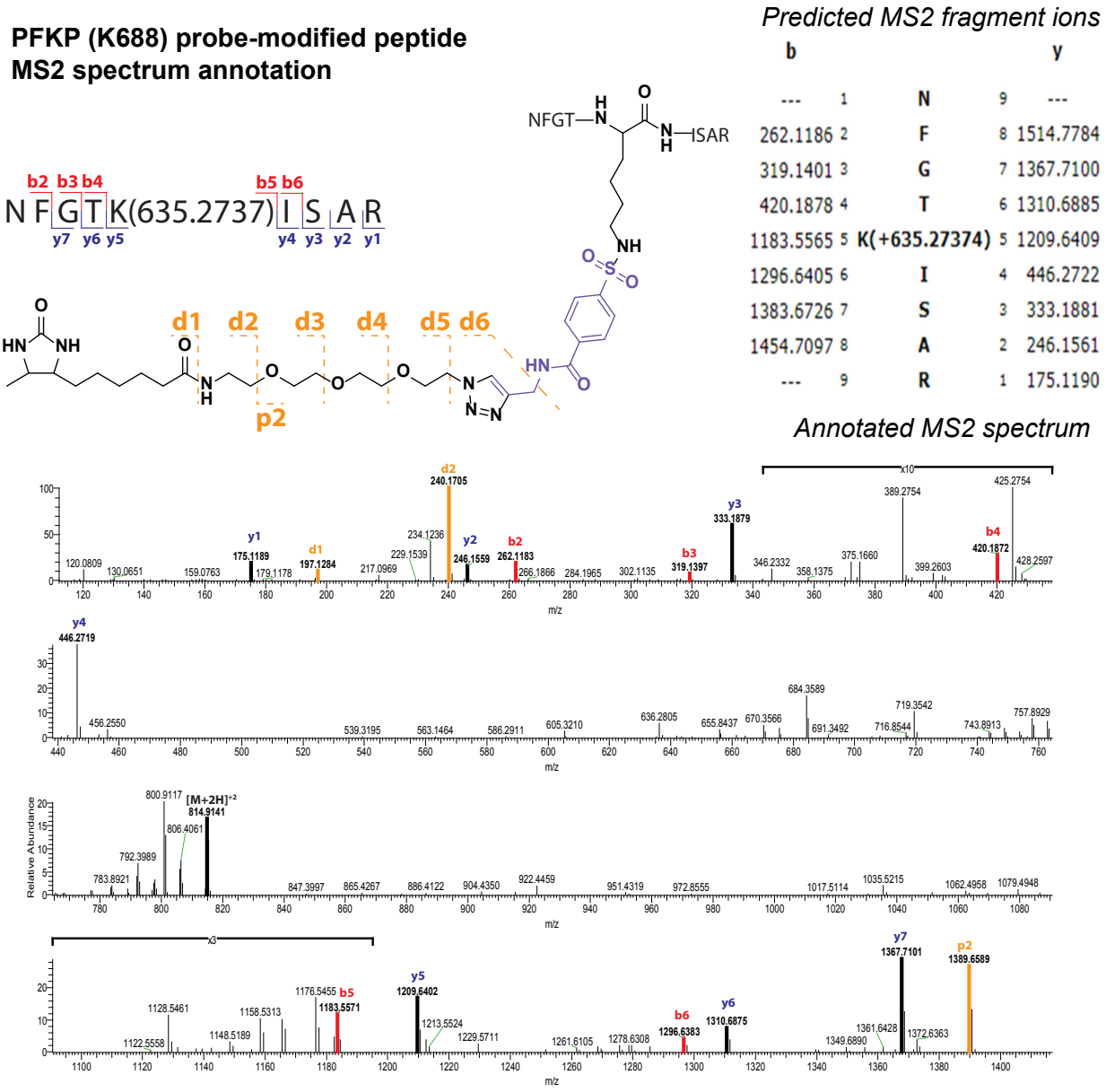

Supplementary Figure 8. **MS2 annotation of the PFKP (K688) HHS-475-modified tryptic peptide**. Left panel: Modified sequence and fragment ion notation of NFGTK*ISAR (residue 684-692) peptide from PFKP. Covalent reaction of HHS-475 with K688 results in a modified lysine (K*) with the addition of +635.2737 Da. Fragmentation of the desthiobiotin-containing tag is also shown. Right panel: predicted MS2 b- and y-fragment ions from CID as determined using Protein Prospector software. Bottom panel: annotation of the MS2 spectrum for the HHS-475-modified PFKP K688 tryptic peptide including fragment ions containing the probe binding site (modified lysine). Data shown are representative of two experiments (*n*=2 biologically independent experiments).

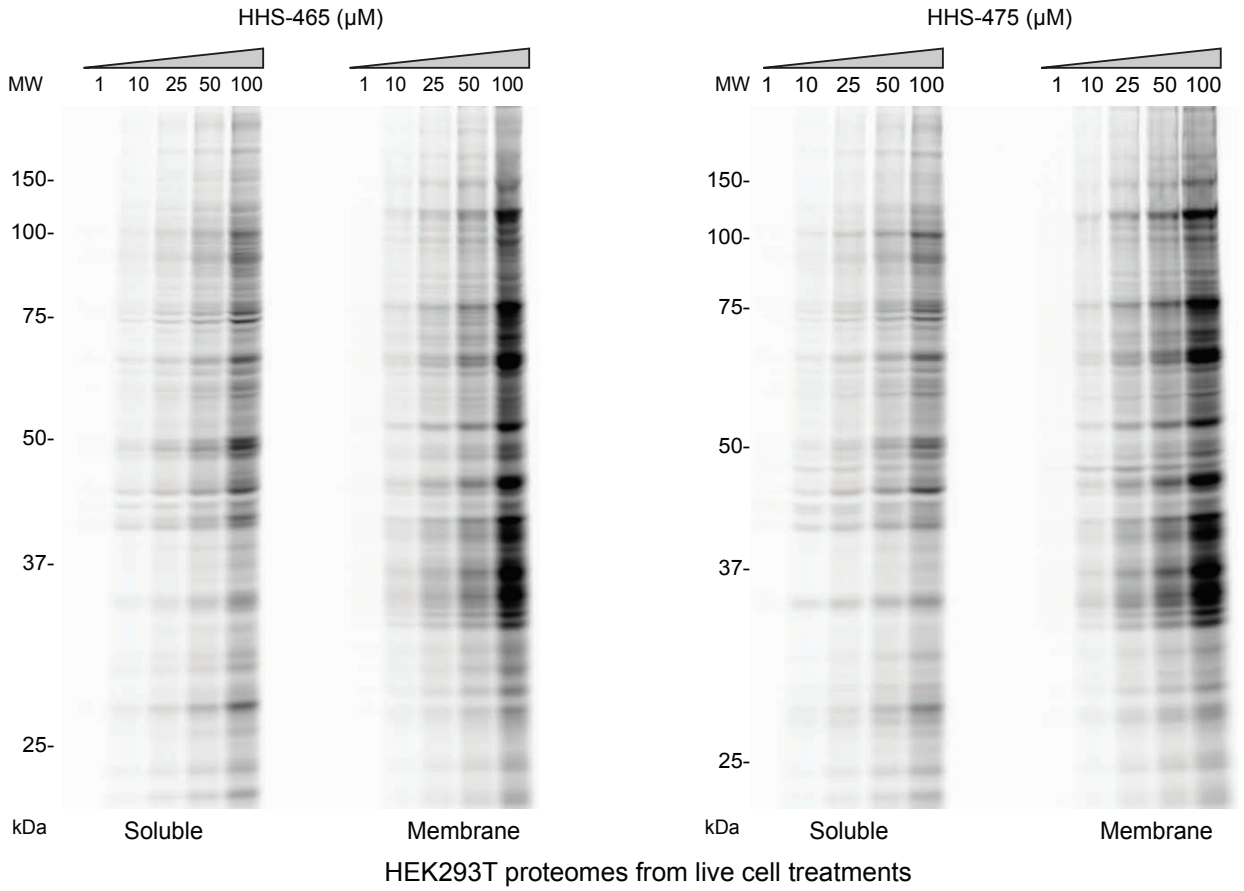

Supplementary Figure 9. **Concentration-dependent labeling of live HEK293T cells treated with SuTEx probes**. HEK293T cells were treated with indicated concentrations of HHS-465 (left panel) or HHS-475 (right panel) for 2 h at 37 °C. After treatment, cells were lysed, probe-modified proteomes (1 mg/mL) subjected to CuAAC with rhodamine-azide followed by SDS-PAGE analysis and in-gel fluorescence scanning. Data shown are representative of two experiments (n=2 biologically independent experiments).

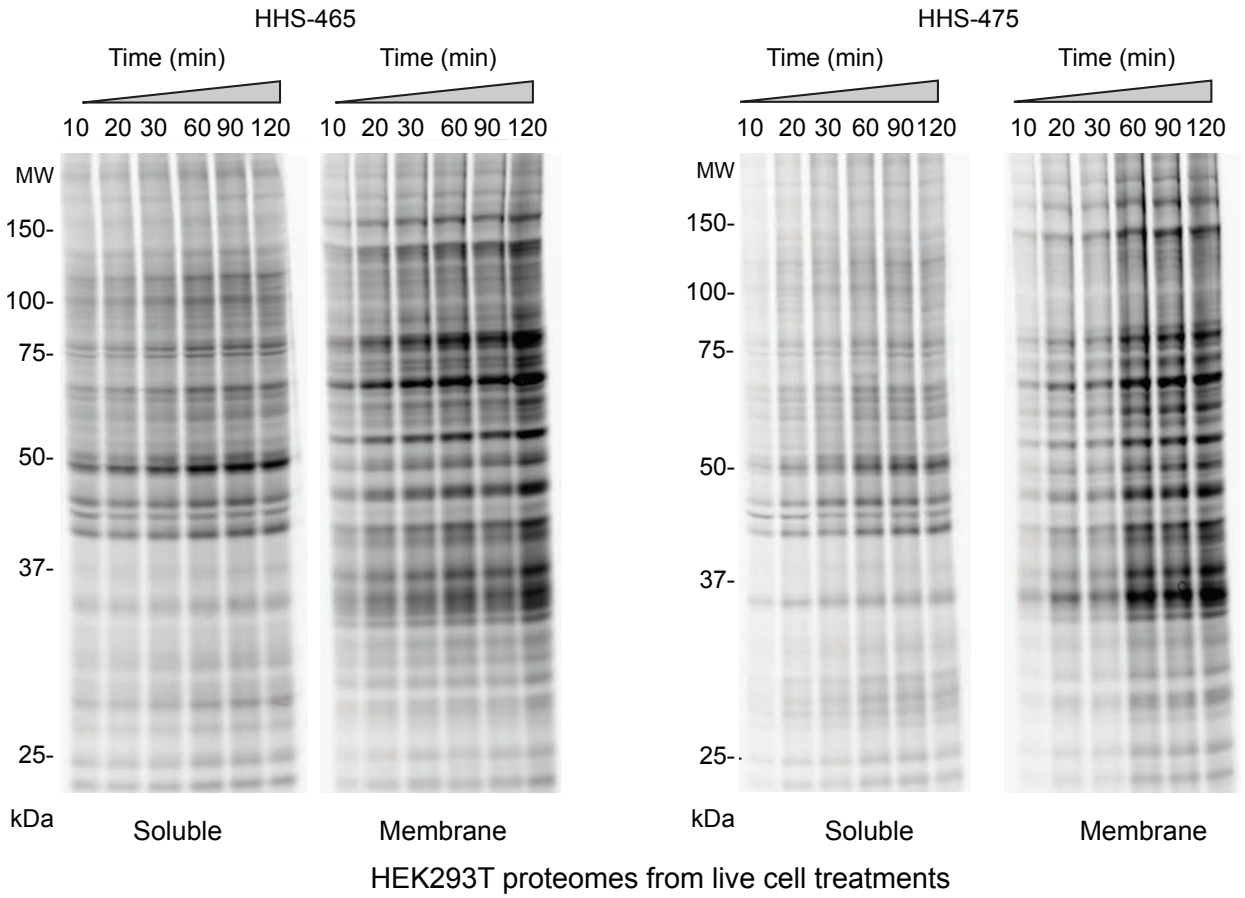

Supplementary Figure 10. **Time-dependent labeling of live HEK293T cells treated with SuTEx probes**. HEK293T cells were treated with 25 μM of HHS-465 (left panel) or HHS-475 (right panel) for the indicated times at 37 °C. After treatment, cells were lysed, and the probe-modified proteomes (1 mg/mL) were subjected to CuAAC with rhodamine-azide followed by SDS-PAGE analysis and in-gel fluorescence scanning. Data shown are representative of two experiments (*n*=2 biologically independent experiments).

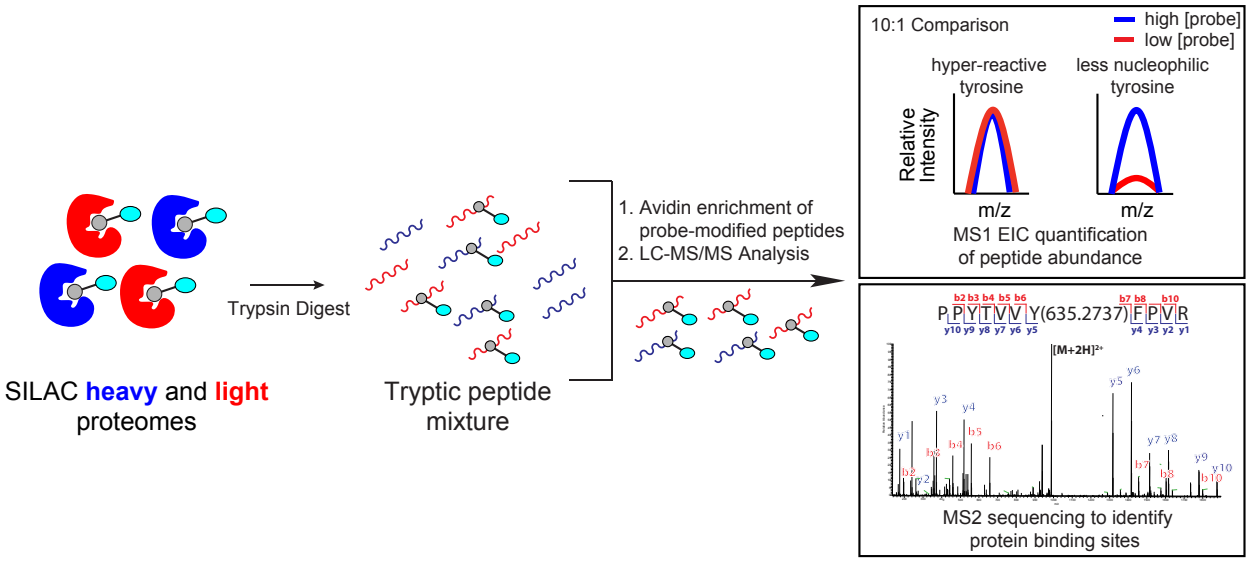

Supplementary Figure 11. **Quantitative chemical proteomics for profiling tyrosine reactivity**. Experimental workflow for quantitative chemical proteomics to measure intrinsic tyrosine nucleophilicity (i.e. reactivity). HEK293T cells were cultured in SILAC media supplemented with either "light" ^{12}C, ^{14}N-labeled lysine and arginine (denoted in red) or "heavy" ^{13}C, ^{15}N-labeled lysine and arginine (denoted in blue). Heavy and light HEK293T proteomes were treated with 250 (high [probe]) or 25 µM (low [probe]) HHS-465, respectively (10:1 comparison). The resulting SILAC ratios (*SR*) were quantified using the area under the curve of MS1 extracted ion chromatograms. Hyper-reactive tyrosines are expected to show equivalent probe labeling intensity at high and low [probe] (left MS1, *SR*~1) while less nucleophilic tyrosines show concentration dependent probe labeling (right MS1, *SR* >>1). A separate experiment where heavy and light proteomes are treated with equivalent [probe] (1:1 comparison) is used as a control for potential false quantifications. See Supplementary Fig. 12 for representative examples. Peptide sequencing and validation of the site of probe binding are determined using MS2 (fragmentation) spectra (bottom panel).

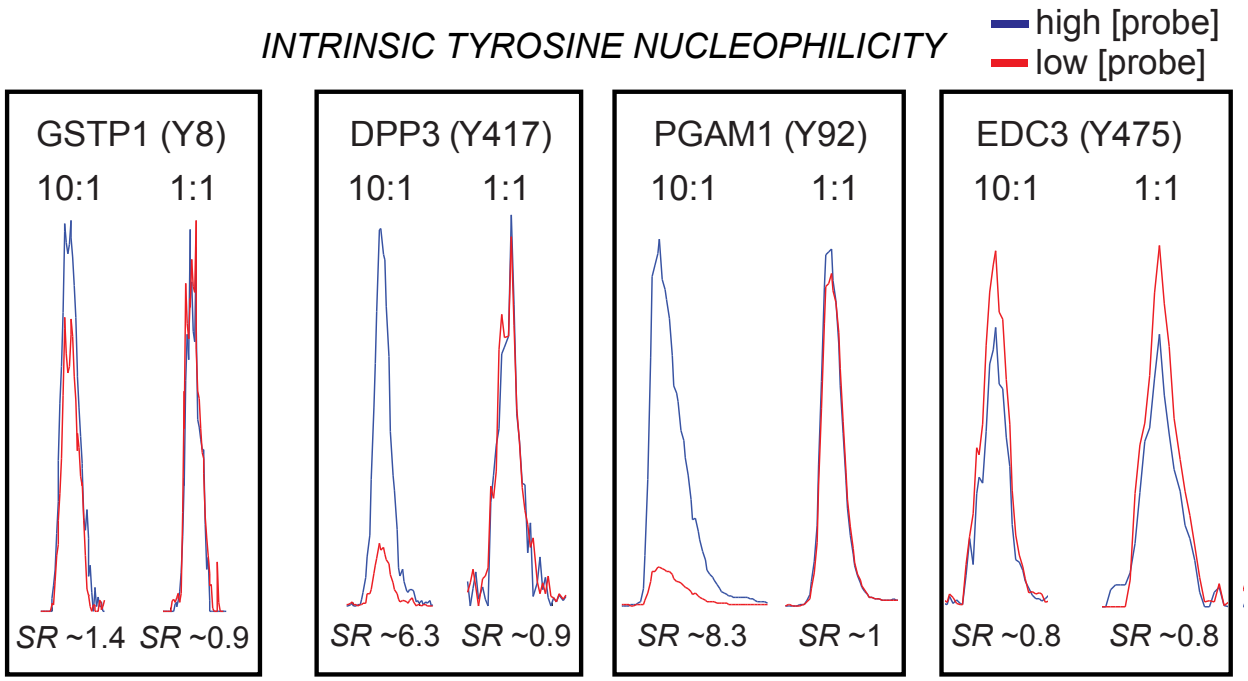

Supplementary Figure 12. **Quantitative analysis of tyrosine reactivity**. Quantitative comparison of tyrosine nucleophilicity between sites detected in human GSTP1 (Y8), DPP3 (Y417), PGAM1 (Y92), and EDC3 (Y475). Heavy and light MS1 extracted ion chromatograms were used to calculate the SILAC ratio (*SR*) for 10:1 and 1:1 probe (HHS-465) comparisons. Data shown are representative of two experiments (n=2 biologically independent experiments).

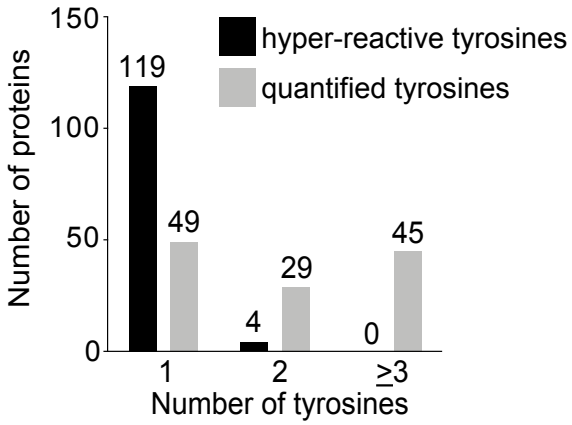

Supplementary Figure 13. Bar plot of the number of hyper-reactive (high nucleophilicity) and quantified tyrosines per protein that contained at least a single hyper-reactive tyrosine. Data shown are representative of two experiments (n=2 biologically independent experiments).

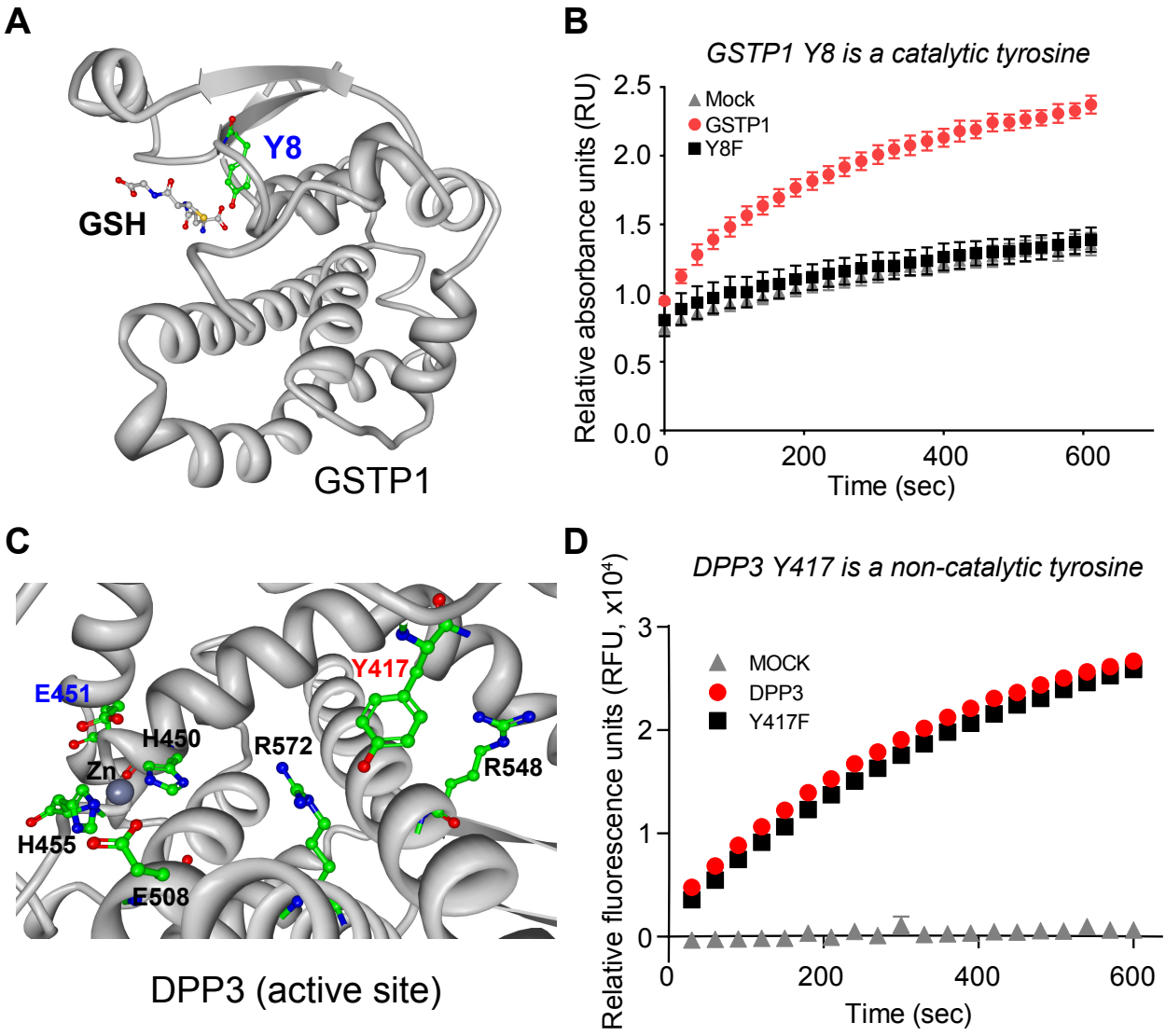

Supplementary Figure 14. **SuTEx probes target reactive catalytic and non-catalytic tyrosines of enzymes**. A) Crystal structure of human GSTP1 (grey, PDB accession code 6GSS) shows tyrosine 8 (Y8) is located in the GSH binding site. B) Loss of biochemical activity in GSTP1 Y8F mutant supports tyrosine 8 as a catalytic residue. Biochemical activity of recombinant GSTP1-HEK293T proteomes (1 mg/mL) was assessed using a substrate assay measuring GSTP1-catalyzed conjugation of GSH to BDNB (10 min, 37 °C). See Supplementary Fig. 15 for additional details. Data are shown as mean ± s.e.m,; *n*=7 biologically independent experiments. C) Crystal structure of human DPP3 (grey, PDB accession code 3FVY) showing location of residues involved in zinc metal binding (H450, H455, E508), the catalytic glutamate (E451), and a non-catalytic tyrosine 417 (Y417) identified by SuTEx. Positively-charged arginines (R548, R572) are found in close proximity to Y417. D) Recombinant DPP3- and Y417F mutant-HEK293T soluble proteomes (1 mg/mL) showed comparable activity in a peptidase substrate assay (Supplementary Fig. 16) supporting Y417 as a non-catalytic tyrosine. Data are show as mean ± s.e.m,; *n*=4 biologically independent experiments.

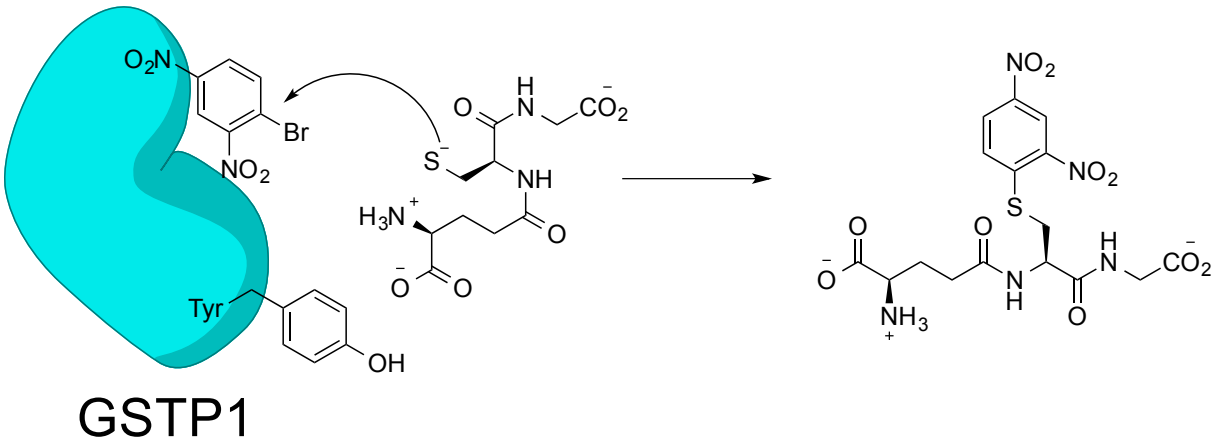

Supplementary Figure 15. **GSTP1 biochemical substrate assay**. GSTP1 catalytic activity was evaluated by monitoring transfer of glutathione (GSH) to 1-bromo-2,4-dinitrobenzene (BDNB), which produces a dinitrophenyl thioether that can be detected spectrophotometrically by measuring absorbance at 340 nm.

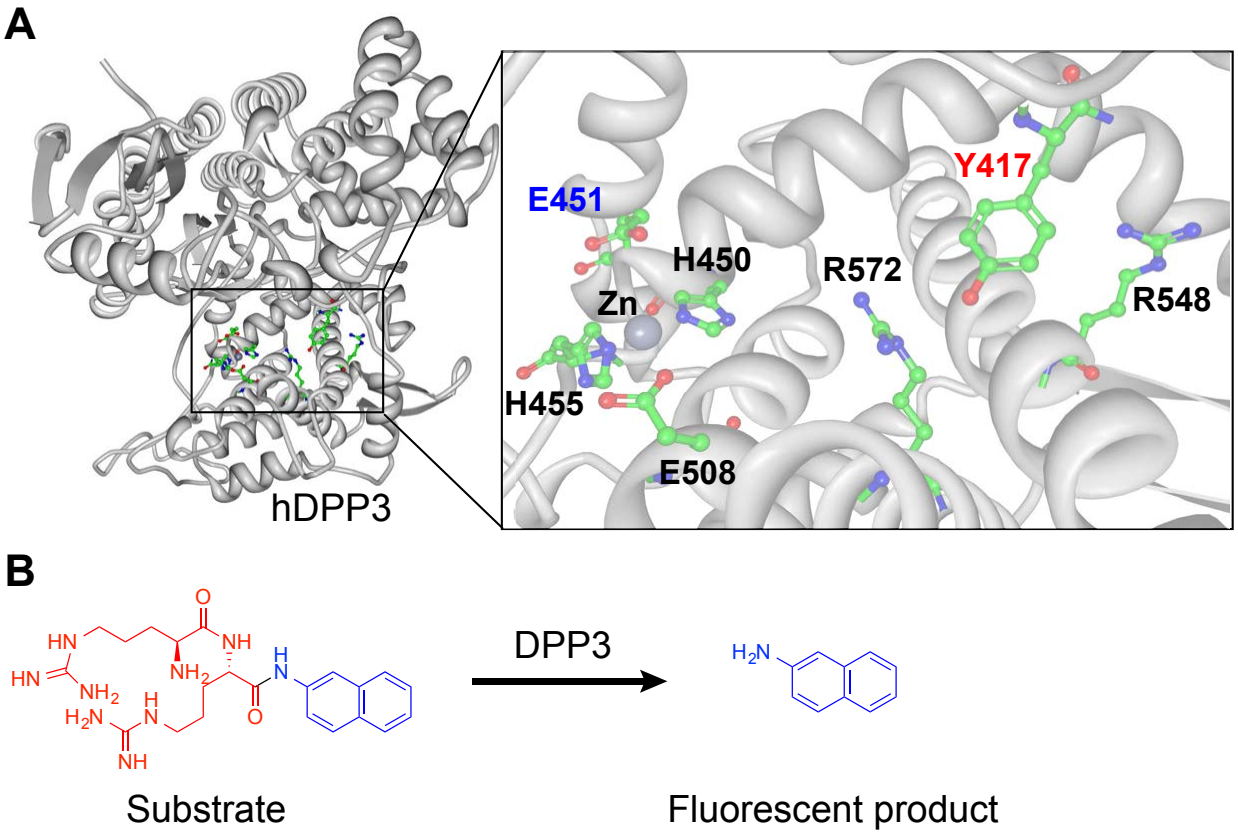

Supplementary Figure 16. **Substrate assay for evaluating DPP3 tyrosine 417 mutant**. A) Crystal structure of human DPP3 (grey, PDB accession code 3FVY) showing location of residues involved in zinc metal binding (H450, H455, E508), the catalytic glutamate (E451), and a non-catalytic tyrosine 417 (Y417) identified by SuTEx. Positively-charged arginines (R548, R572) are found in close proximity to Y417. B) DPP3 cleaves Arg-Arg β-naphthylamide substrate to release the colored naphthylamide product that can be detected spectrophotometrically by measuring fluorescence at 450 nm.

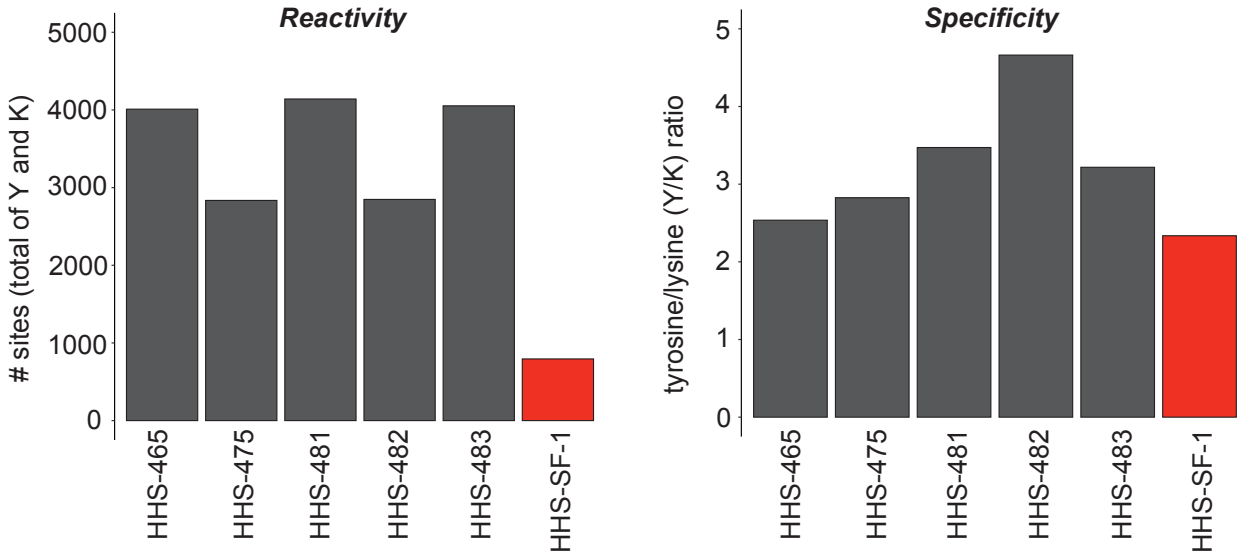

Supplementary Figure 17. **Bar plot depiction of global tyrosine reactivity and selectivity of SuTEx and SuFEx probes shown in Fig 4A**.

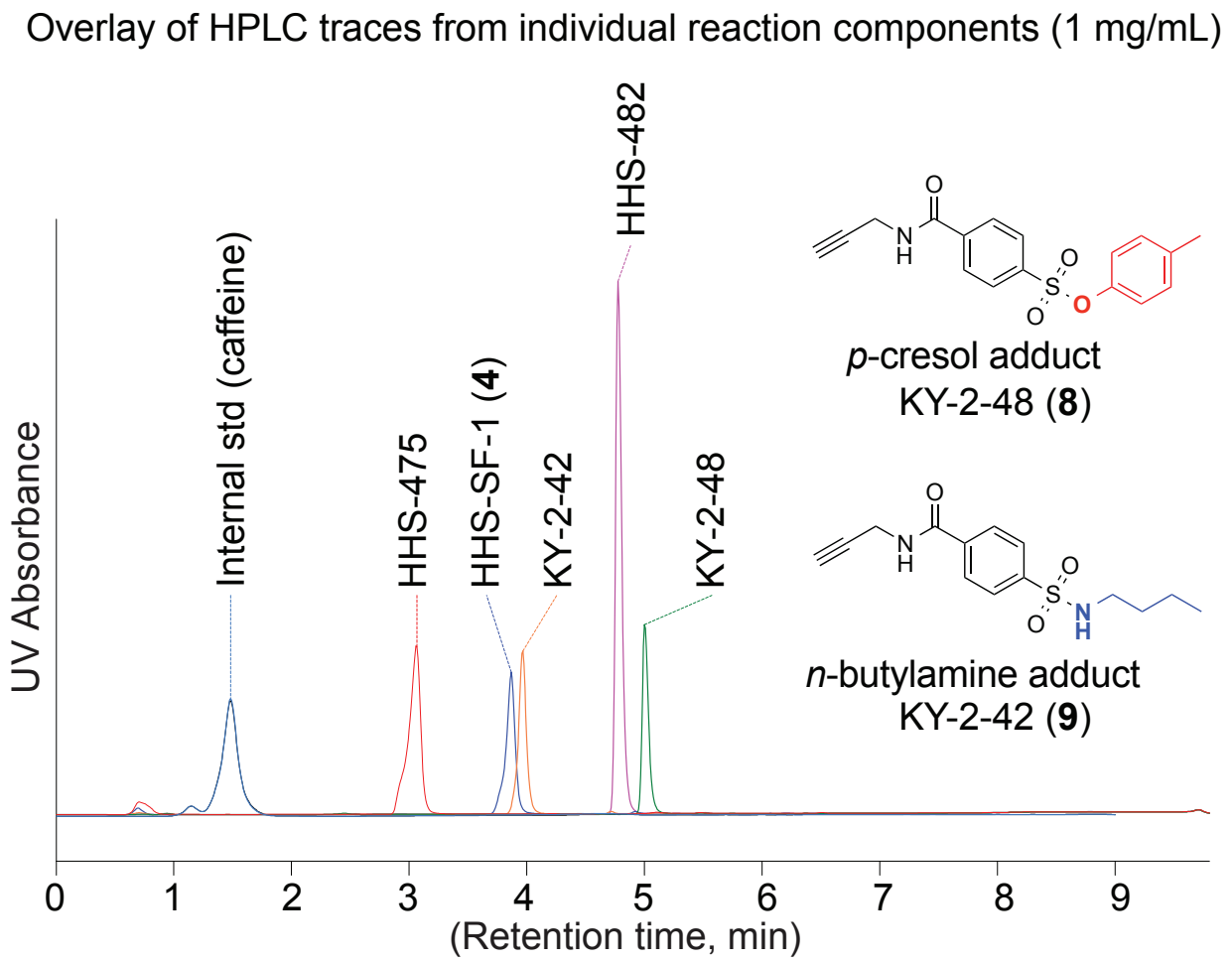

Supplementary Figure 18. Overlay of individual HPLC traces at 1 mg/mL concentrations to show chromatographic resolution of reaction components: caffeine (sky blue), HHS-475 (red), HHS-SF-1 (blue), KY-2-42 (orange, *n*-butylamine-probe adduct), HHS-482 (pink), KY-2-48 (green, *p*-cresol-probe adduct). Caffeine was spiked into each sample as an internal standard to control for run-to-run variations in HPLC analysis (UV detection at 254 nm) of SuTEx and SuFEx reactions. Data shown are representative of two independent experiments (n=2).

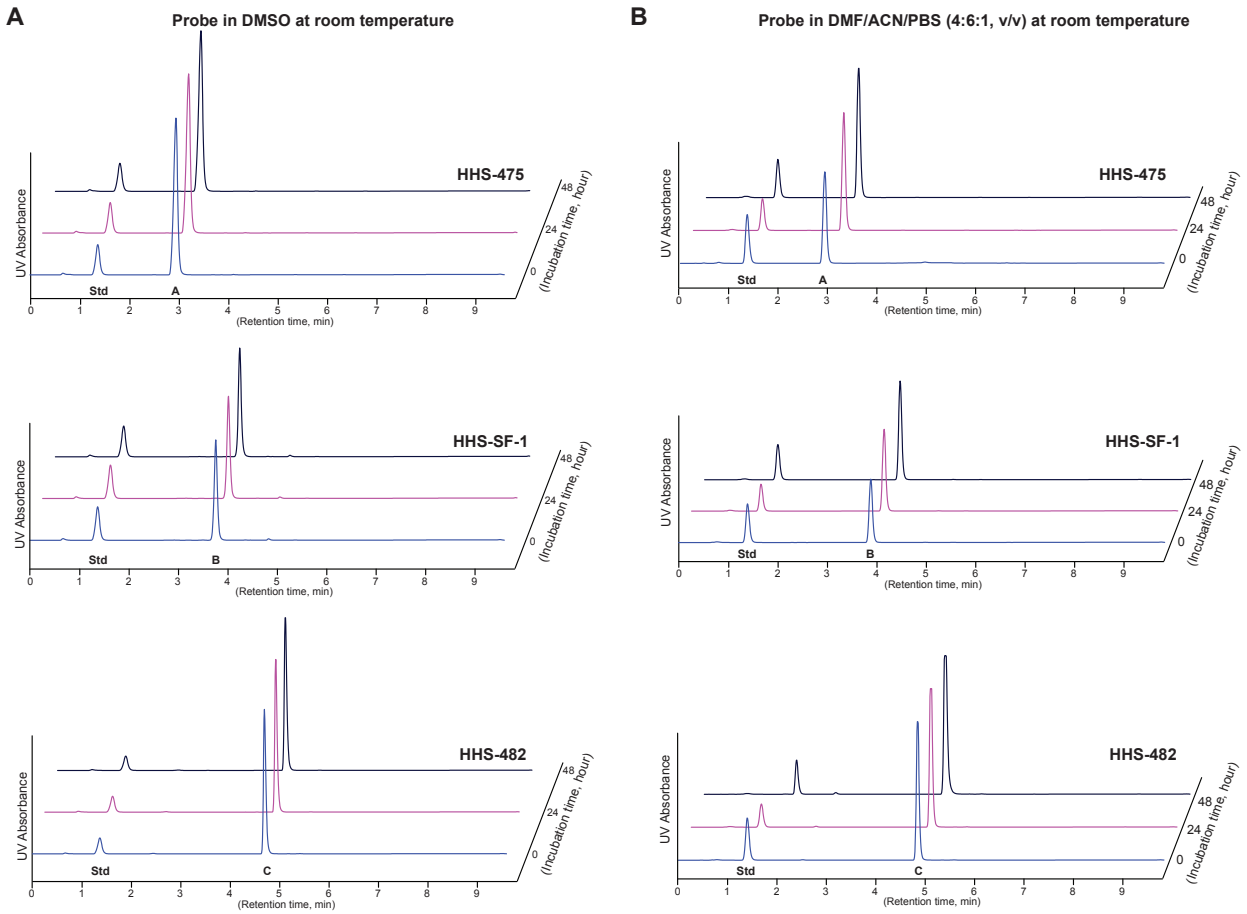

Supplementary Figure 19. **Stability of sulfonyl probes in DMSO and aqueous/solvent mixtures**. DMSO solutions of HHS-475 (20 mM), HHS-SF-1 (20 mM), and HHS-482 (10 mM) were prepared and HPLC analysis of these probes measured at the indicated time points. Negligible degradation, as judged by reduction of probe signal, was observed after 24- and 48-hours incubation in DMSO or DMF:ACN:PBS (4:6:1, (v/v)) at room temperature. See Supplementary Methods for additional details of the stability assay. DMSO: dimethyl sulfoxide, DMF: dimethylformamide, ACN: acetonitrile, PBS: phosphate-buffered saline. Data shown are representative of three independent experiments (*n*=3).

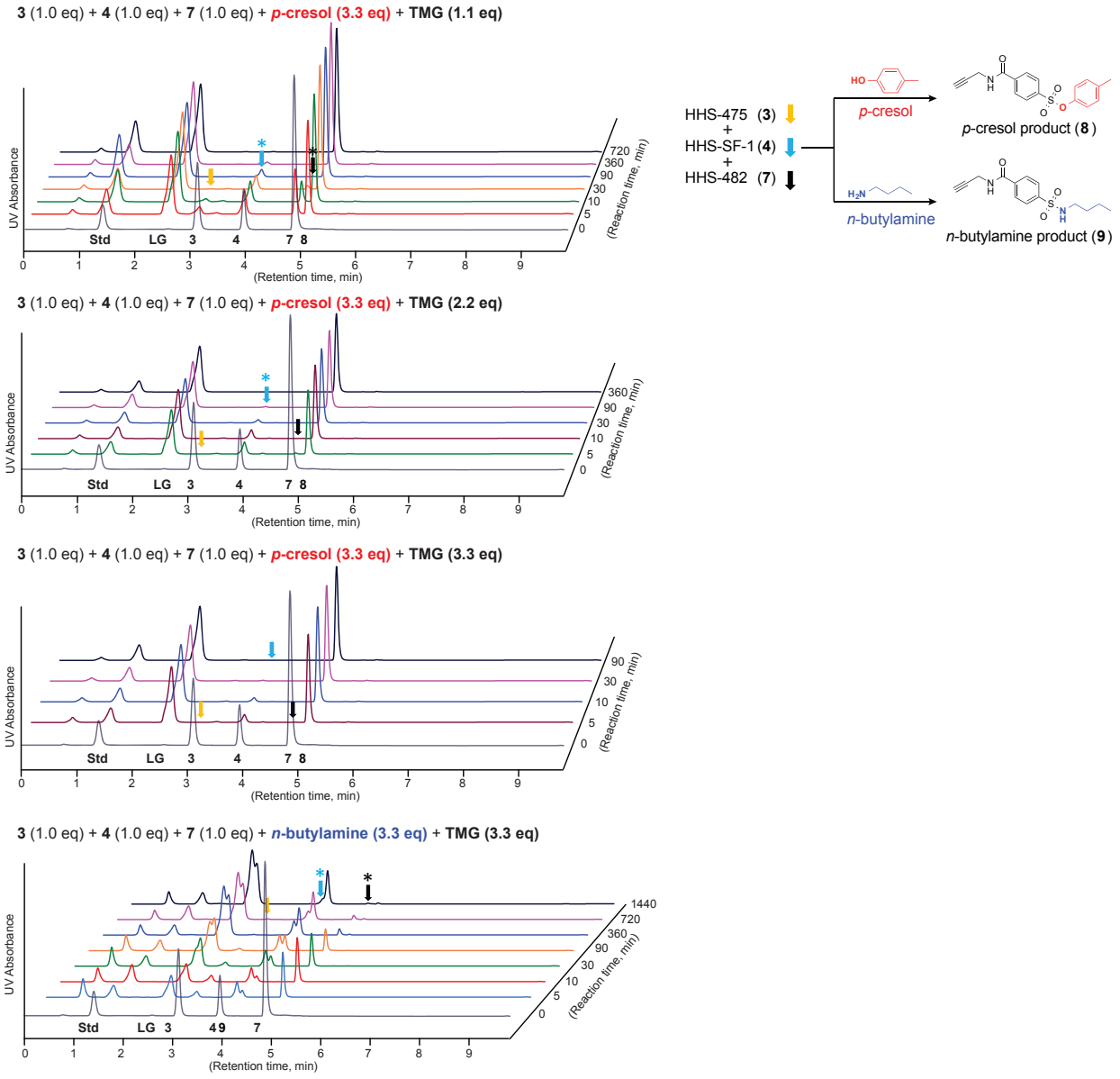

Supplementary Figure 20. **Comparison of SuTEx and SuFEx reactivity against nucleophiles in solution**. Time-dependent reactions between *p*-cresol or *n*-butylamine with a mixture of HHS-475 (peak 3), HHS-SF-1 (peak 4), and HHS-482 (peak 7) under increasing amounts of TMG base. Formation of the corresponding *p*-cresol-probe (peak 8) or *n*-butylamine-probe products (peak 9) was confirmed by retention times that matched the synthetic standards KY-2-48 and KY-2-42, respectively (Supplementary Fig. 18). Std: internal standard, Caffeine, LG: leaving group of HHS-482 (3-(4-methoxy phenyl)-1,2,4-triazole) from covalent reaction, TMG: tetramethylguanidine. Data shown are representative of three independent experiments (n=3).

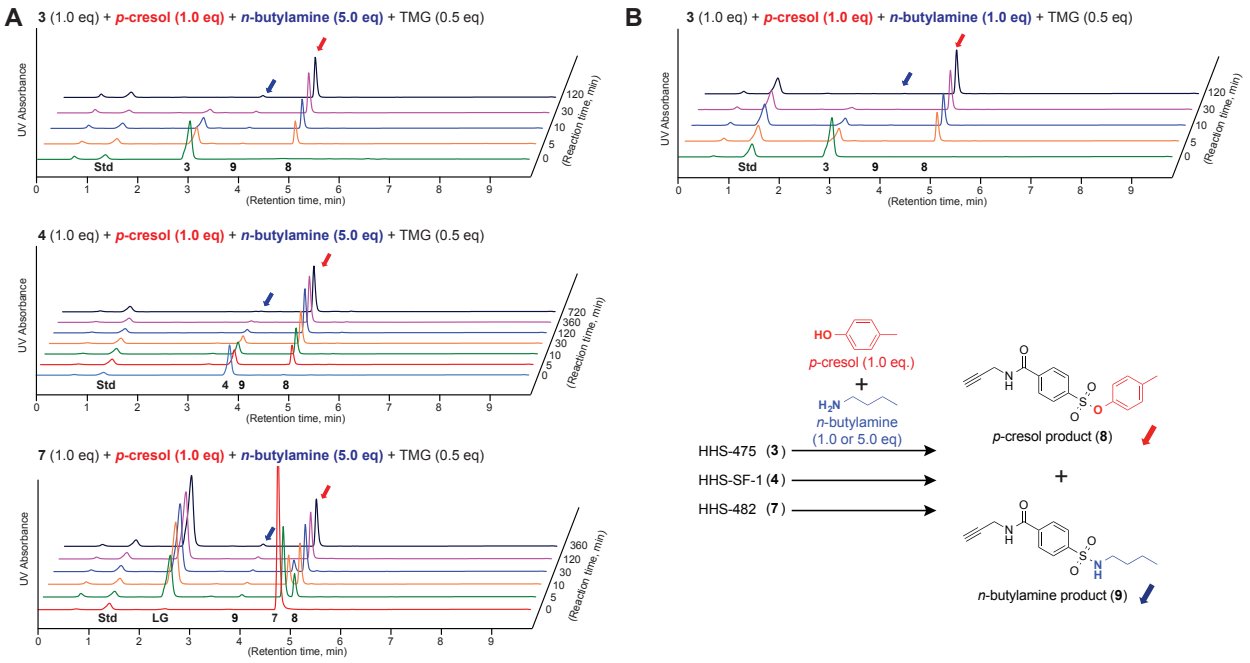

Supplementary Figure 21. **Chemoselectivity of sulfonyl probes against *p*-cresol and *n*-butylamine in solution**. Reaction of individual sulfonyl probes against a mixture of *n*-butylamine and *p*-cresol mixture. Condition A shows the traces of a mixture of *n*-butylamine and *p*-cresol of 5:1 ratio under catalytic TMG (0.5 equivalents). Condition B entails the reaction of the sulfonyl probes with a mixture of equivalent amounts of *n*-butylamine and *p*-cresol under catalytic amount of TMG (0.5 equivalents). Red arrows show formation of *p*-cresol-probe product (peak 8) and blue arrows show formation of *n*-butylamine-probe product (peak 9) under respective reaction conditions. Std: internal standard, caffeine, LG: leaving group of HHS-482 (3-(4-methoxy phenyl)-1,2,4-triazole) from covalent reaction, TMG: tetramethylguanidine. Data shown are representative of three independent experiments (*n*=3).

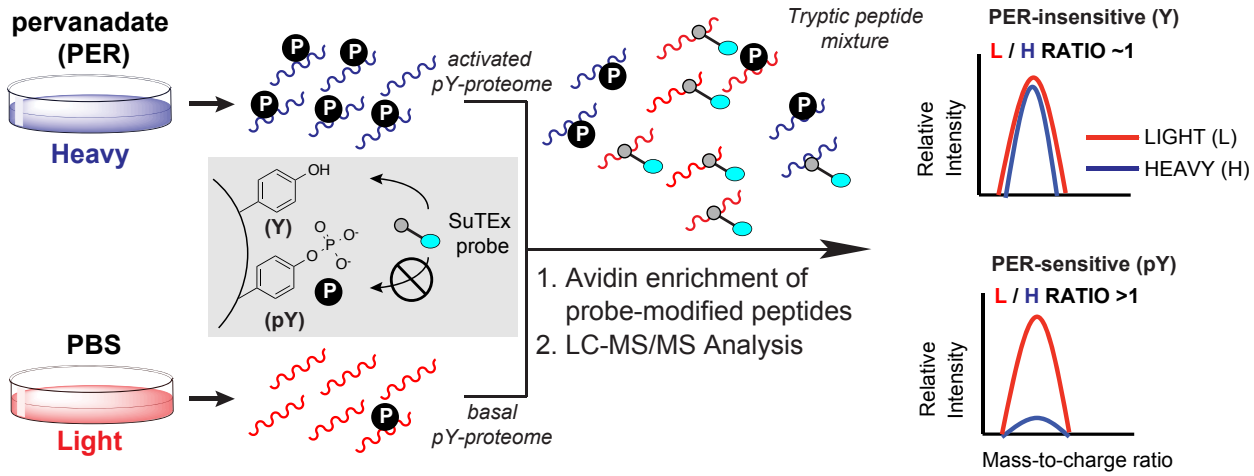

Supplementary Figure 22. Schematic of a SuTEx platform for global tyrosine phosphoproteomic studies. Activation of tyrosine phosphorylation (pY) using a general tyrosine phosphatase inhibitors (pervanadate) will reduce availability of tyrosines (Y) for SuTEx probe labeling, which can be readout by quantitative chemical proteomics (SILAC).

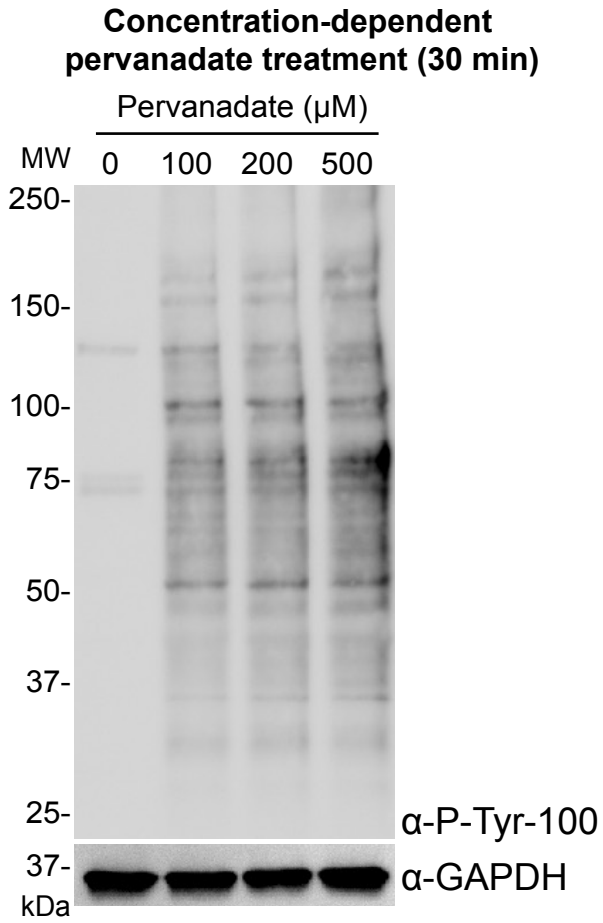

Supplementary Figure 23. **Concentration-dependent activation of global tyrosine phosphorylation**. A549 cells were treated with vehicle (PBS) or pervanadate at the indicated concentrations for 30 min followed by cell lysis in PBS + protease and phosphatase inhibitors. Activation of global tyrosine phosphorylation was assessed by western blot analysis with a phospho-tyrosine monoclonal antibody (P-Tyr-100). Equivalent protein loading was confirmed using an antibody against GAPDH. Full image of GAPDH blot is shown in Supplementary Fig. 29. Data shown are representative of two experiments (n=2 biologically independent experiments).

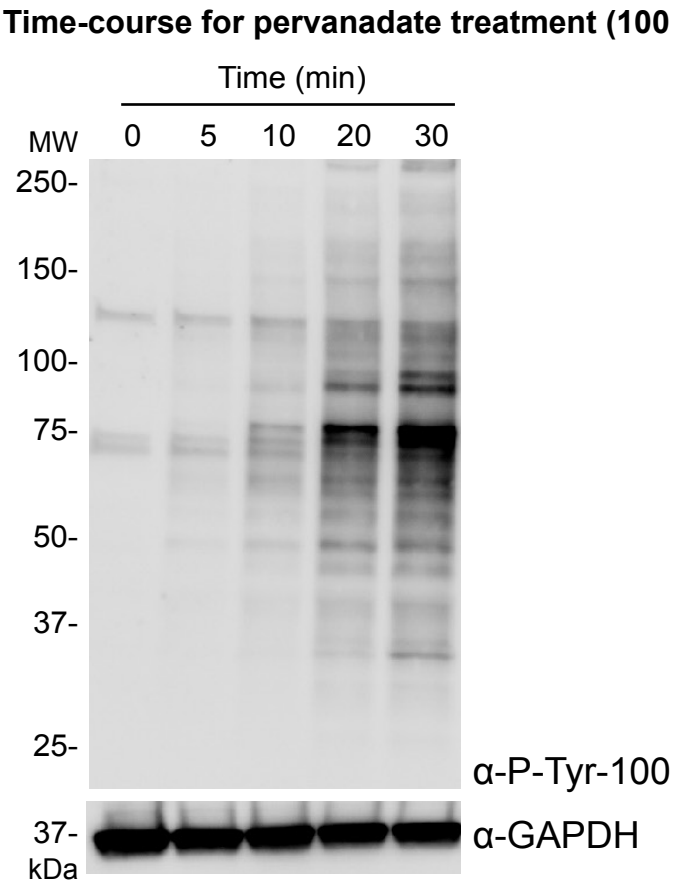

Supplementary Figure 24. **Time-dependent activation of global tyrosine phosphorylation**. A549 cells were treated with vehicle (PBS) or pervanadate (100 μM) and lysed in PBS + protease and phosphatase inhibitors at the indicated time points. Global tyrosine phosphorylation activation measured by western blot analysis using a phospho-tyrosine monoclonal antibody (P-Tyr-100). Equivalent protein loading was confirmed using an antibody against GAPDH. Full image of GAPDH blot is shown in Supplementary Fig. 30. Data shown are representative of two experiments (*n*=2 biologically independent experiments).

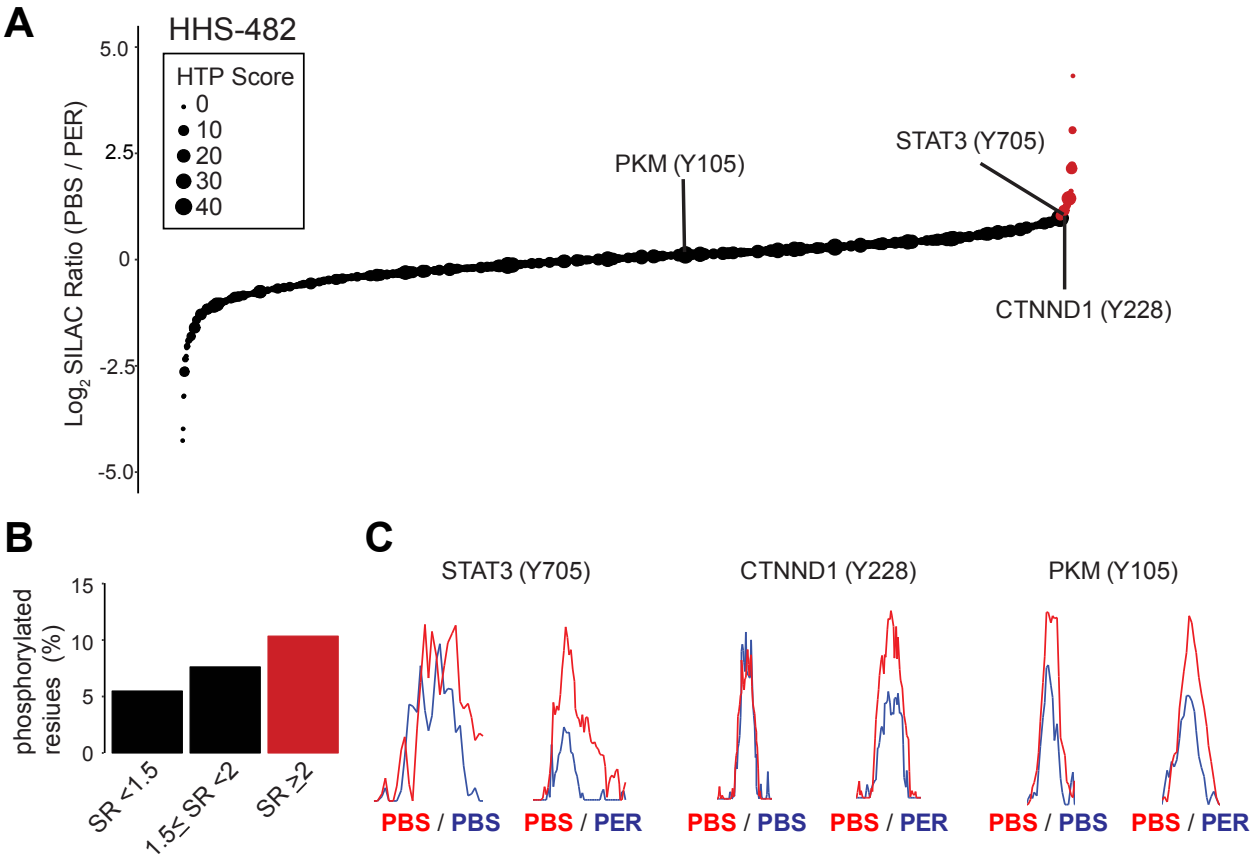

Supplementary Figure 25. **Chemical phosphotyrosine-proteomics by HHS-482**. (A) Plot of HHS-482-modified tyrosine sites (represented by individual circles) as a function of SILAC ratios (*SR,* light (PBS)/heavy (pervanadate or PER)). Size of circles reflect the number of phosphotyrosine high throughput annotations on PhosphoSitePlus (HTP score). Tyrosine sites were further segregated into pervanadate-insensitive (black circles) and -sensitive (red circles) groups based on *SR* <2 or ≥2, respectively. Soluble proteomes from pervanadate activated-A549 cells were labeled with HHS-482 (100 μM) for 30 min at 37 °C. (B) Bar plot showing trend towards increased phosphotyrosine annotation (HTP ≥10) in tyrosine sites with enhanced pervanadate sensitivity. (C) Validation that blockade of HHS-482 labeling of individual tyrosine sites on STAT3 (Y705), CTNND1 (Y228), and PKM (Y105) coincides with increased phosphorylation at respective sites with pervanadate activation (see Fig 7F). See Table S1 for *SR* values of tyrosines sites detected by chemical proteomics. Data shown are representative of two experiments (*n*=2 biologically independent experiments).

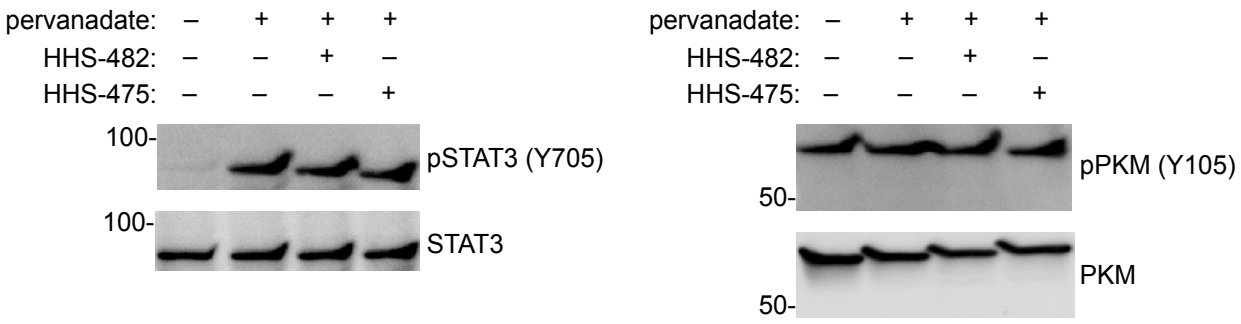

Supplementary Figure 26. **SuTEx probe treatment of proteomes from pervanadate-treated cells does not displace phospho-tyrosines**. A549 cells were treated with vehicle (PBS) or pervanadate (100 μM, 30 min) followed by lysis in PBS + protease and phosphatase inhibitors. Proteomes from pervanadate-treated cells were treated with either HHS-482 or HHS-475 (100 μM of SuTEx probe) for 30 min at 37 ˚C followed by western blot analysis of individual tyrosine sites on STAT3 (Y705) and PKM (Y105). Treatment with either HHS-482 or HHS-475 did not affect phosphotyrosine signals indicating that SuTEx probes do not non-specifically displace phosphates from tyrosines. See Methods for additional details of western blot analyses. Full image of blots are shown in Supplementary Fig. 31. Data shown are representative of two experiments (*n*=2 biologically independent experiments).

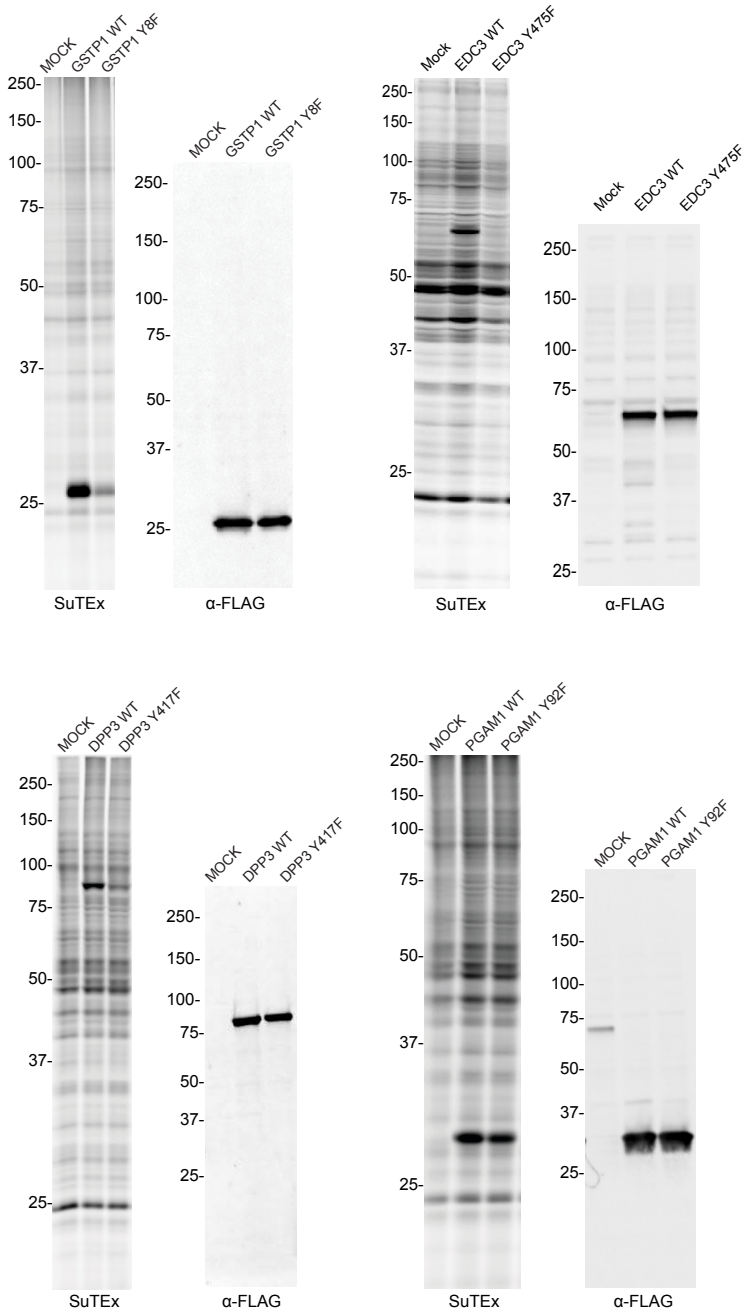

Supplementary Figure 27. Full images of gels and blots related to Fig. 3d.

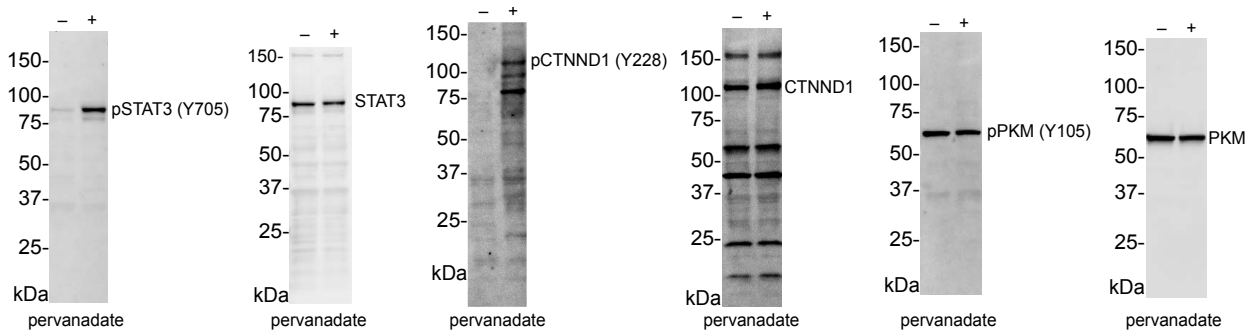

Supplementary Figure 28. Full images of blots related to Fig. 6e.

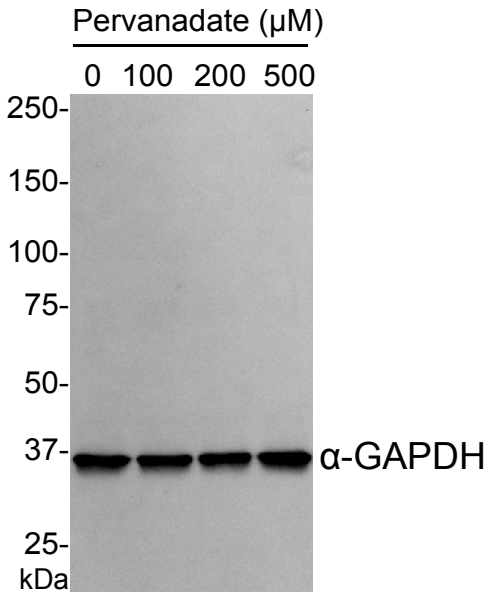

Supplementary Figure 29. Full image of GAPDH blot related to Supplementary Fig. 23.

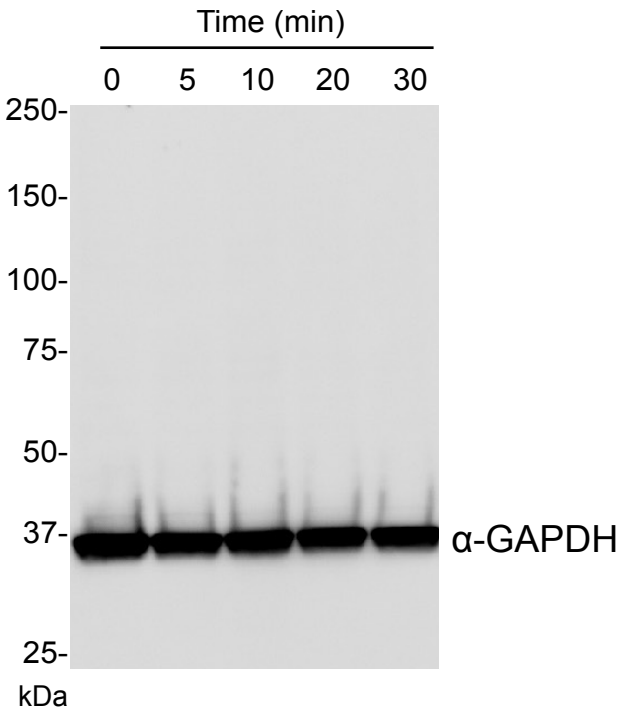

Supplementary Figure 30. Full image of GAPDH blot related to Supplementary Fig. 24.

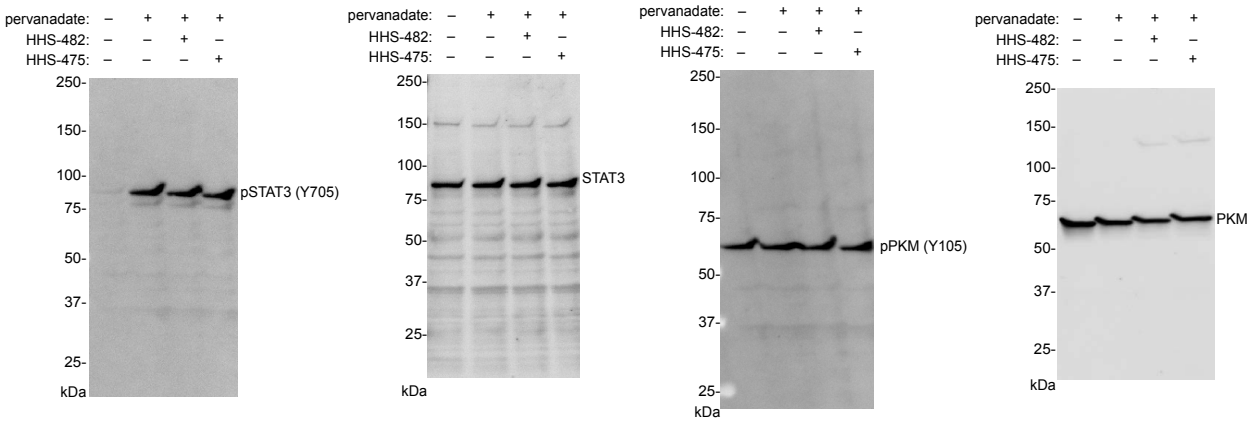

Supplementary Figure 31. Full images of blots related to Supplementary Fig. 26.

SUPPLEMENTARY DATASETS

Supplementary Dataset 1.
A) Number of unique labeled tyrosine sites modified by different SuTEx probes either *in vitro*, *in situ* or in aggregate that met our Byonic quality control confidence criteria (score > 300, ppm < 5.0, and specific trypsin cleavage).

B) Number of unique labeled proteins modified by different SuTEx probes either *in vitro*, *in situ* or in aggregate that met our Byonic quality control confidence criteria.

C) Tyrosine reactivity ratios. SILAC ratios (*SR*) of HEK293T proteomes treated *in vitro* with either 25 μM (SILAC light) or 250 μM (SILAC heavy) HHS-465. Ratios are listed as heavy over light (10:1 comparison).

D) Modified tyrosines from HEK293T or Jurkat cells treated *in situ* with HHS-465 or HHS-475 that 1) met our Byonic quality control confidence criteria and 2) have been reported as phosphorylation sites in at least 10 independent high throughput experiments according to the PhosphositePlus database. Complete PhosphositePlus database entry is listed.

E) Probe-modified sites in the RNA recognition motif (RRM) domain of serine/arginine-rich splicing factors (SRSF). SRSF proteins containing a probe-modified tyrosine within the RRM domain from HEK293T or Jurkat cells treated *in situ* with HHS-465 or HHS-475 that met our Byonic quality control confidence criteria.

F) SILAC ratios of soluble proteomes (Uniprot ID_tyrosine site) from PBS (light)/pervanadate (heavy) treatments of A549 cells labeled with HHS-475.

G) SILAC ratios of soluble proteomes (Uniprot ID_tyrosine site) from PBS (light)/pervanadate (heavy) treatments of A549 cells labeled with HHS-482.

H) Reactivity of SuTEx and SuFEx probes. Area under the curve values for internal standard, reactant, and product peaks from HPLC solution reactivity studies depicted in Fig 5 and Supplementary Figure 20 are included.

I) HPLC data for *p*-cresol reaction with individual sulfonyl probes. Data includes the area under the curve values for internal standard, reactant, and product peaks.

J) Stability studies of SuTEx and SuFEx probes. The area under the curve values for sulfonyl probe and internal standard peaks depicted in Supplementary Figure 19 are included.

K) Selectivity of individual probes against a mixture of *p*-cresol and *n*-butylamine. Area under the curve values for internal standard, reactant, and product peaks from HPLC solution reactivity studies depicted in Supplementary Figure 21 are included.